

Mesonic dynamics and QCD phase transition

Shi Yin,¹ Rui Wen,¹ and Wei-jie Fu^{1,*}

¹*School of Physics, Dalian University of Technology, Dalian, 116024, P.R. China*

We study the finite temperature and density two flavor quark-meson model under the functional renormalisation group. The effect of broken $O(4)$ -symmetry of the wave function renormalisation and expansion point of effective potential on the thermodynamic quantities and baryon number fluctuation are investigate. At the same time, the field dependent Yukawa coupling is also considered. We give results of the pion mass, the quark mass, the trace anomaly, the baryon number fluctuation and the freeze-out curve.

I. INTRODUCTION

The QCD phase structure and the search of the critical end point (CEP) are the most popular research direction in both experimental and theoretical field. The phase transition between the quark gluon plasma (QGP) and hadron is the main research objects. The research of the QGP-hadron phase transition can help us to help us better understand the nature of elementary particles. The experiment to looking for the QGP is being made at the Large Hadron Collider (LHC) and the Relativistic Heavy-Ion Collider (RHIC).

In terms of theoretical research, there many different methods to investigate the QCD phase structure. The most widely studied method is the lattice QCD. A lot of properties of the QCD matter have been discussed under the lattice simulations. Although the lattice theory has the sign problem at high baryon chemical potential, it still gave us plenty of great outcomes. In order to avoid the problem that occurs in lattice calculation, the study of the continuous non-perturbative field theory is in progress at the same time. For example, the Dyson-Schwinger equation. And the Functional Renormalization Group (FRG) is the other good functional approach of the continuous theory. In these ways we can study the behavior of the strong interaction matter under the finite temperature and density better.

This work is done with the low energy effective model under the FRG approach.

The low-energy effective models, e.g. the quark-meson (QM) model [1], Nambu–Jona-Lasinio (NJL) model, and their Polyakov-loop improved variants: PQM and PNJL, are suitable to be employed to study the QCD phase transitions. They have been investigated quite a lot in literatures, see, e.g., [2] for more details. In this work, we adopt the scale-dependent effective action for the two-

flavor PQM model, as follows

$$\Gamma_k = \int_x \left\{ Z_{q,k} \bar{q} \left[\gamma_\mu \partial_\mu - \gamma_0 (\hat{\mu} + ig A_0) \right] q + \frac{1}{2} \left[Z_{\phi,k}^{\parallel} (\partial_0 \phi)^2 + Z_{\phi,k}^{\perp} (\partial_i \phi)^2 \right] + h_k(\rho) \bar{q} (T^0 \sigma + i \gamma_5 \vec{T} \cdot \vec{\pi}) q + V_k(\rho) - c\sigma \right\}, \quad (1)$$

with $\mu = (0, 1, \dots, 3)$ and $i = (1, 2, 3)$. In Eq. (1) we have used notation $\int_x = \int_0^{1/T} dx_0 \int d^3x$, where the imaginary time formalism for the field theory at finite temperature is used, and the temporal length reads $\beta = 1/T$. Apparently, when the temperature is nonzero, the $O(4)$ -symmetry in the Euclidean space is broken into that of $\mathbb{Z}_2 \otimes O(3)$, which leads to the split of the magnetic and electric components of correlations functions. They correspond to the components transversal and longitudinal to the heat bath, respectively. In this work, we take this split into account in the two-point correlation function for the mesons, as shown in the second line on the r.h.s. of Eq. (1), where $Z_{\phi,k}^{\parallel}$ and $Z_{\phi,k}^{\perp}$ indicate the longitudinal and transversal wave function renormalizations for the temporal and spacial components, respectively.

The reason why we concentrate on the split of the wave function renormalization especially for the mesons is due to the facts as follows. Firstly, in comparison to the quark wave function renormalization $Z_{q,k}$ and the scale dependent Yukawa coupling h_k in Eq. (1), it is found that the meson wave function renormalization $Z_{\phi,k}$ plays the most significant role beyond the local potential approximation (LPA) [2, 3]. In the LPA, the propagators are classical, i.e., $Z_{q,k} = Z_{\phi,k} = 1$ and the Yukawa coupling h is a constant and independent of the scale k . Secondly, In Ref. [4] calculations based on the full momentum-dependent two-point correlation functions of mesons are compared with those from LPA and LPA', and here in LPA' a momentum-independent $Z_{\phi,k}$ is included, and it is found that there is a good agreement between the full momentum calculation and the LPA', while not LPA, which indicates that the dispersion relation for the meson, resulting from a scale dependent $Z_{\phi,k}$, have already captured most momentum dependence of the two-point correlation function.

* wjfu@dlut.edu.cn

Considering the importance of the wave function renormalization for the mesons and the success of LPA', in this work we would like to investigate the effects of the splitting of $Z_{\phi,k}$ in the LPA' as shown in Eq. (1), which is a natural choice at finite temperature as discussed above. Furthermore, we will also study the interplay between the splitting of $Z_{\phi,k}$ and other truncation approaches, e.g., the field dependent Yukawa coupling $h_k(\rho)$ which encodes higher order quark-meson scattering processes [2], fixed point expansion for the effective potential $V_k(\rho)$ in Eq. (1) versus the physical point expansion, etc. Their influences on the QCD phase transition and observables, e.g. fluctuations of the baryon number, will be investigated in detail.

II. FUNCTIONAL RENORMALIZATION GROUP AND FLOW EQUATIONS

To proceed, we describe other notations in the effective action in Eq. (1). $\phi = (\sigma, \vec{\pi})$ is a meson field with four components. The effective potential $V_k(\rho)$ with $\rho = \phi^2/2$ is $O(4)$ invariant and the $c\sigma$ breaks the chiral symmetry explicitly. The mesons interact with quarks through the scalar and pseudo-scalar channels with a mesonic field dependent Yukawa coupling $h_k(\rho)$, and T^0 and T^i are the generators in the flavor space with the convention as follows: $\text{Tr}(T^i T^j) = \frac{1}{2}\delta^{ij}$ and $T^0 = \frac{1}{\sqrt{2N_f}}\mathbb{1}_{N_f \times N_f}$ with $N_f = 2$. Besides the wave function renormalization for the meson, we also introduce one for the quark, i.e., $Z_{q,k}$. Since it plays a minor role in the chiral dynamics in comparison to $Z_{\phi,k}$, the splitting of $Z_{q,k}$ into the transversal and longitudinal components are neglected for simplicity in calculations. Finally, $\hat{\mu} = \text{diag}(\mu_u, \mu_d)$ in the first line on the r.h.s. of Eq. (1) denotes the matrix of the quark chemical potential, and $\mu = \mu_u = \mu_d$ is assumed in the following unless stating specifically. A_0 is the temporal gluon background field, through which the Polyakov dynamics is taken into account.

The renormalization group (RG) scale k in Eq. (1) is an infrared cutoff, below which quantum fluctuations are suppressed in the effective action. The evolution of the effective action with k is described by the Wetterich equation [5], which reads

$$\partial_t \Gamma_k[\Phi] = \frac{1}{2} \text{Tr}(G_{\phi\phi,k} \partial_t R_k^\phi) - \text{Tr}(G_{q\bar{q},k} \partial_t R_k^q), \quad (2)$$

with the RG time $t = \ln(k/\Lambda)$ and the initial ultraviolet (UV) cutoff Λ , where R_k^ϕ and R_k^q are the regulators for the meson and quark fields, respectively, and they are given in Eqs. (B1) and (B2). The scale dependent meson and quark propagators are given by

$$G_{\phi\phi/q\bar{q}}[\Phi] = \left(\frac{1}{\frac{\delta^2 \Gamma_k[\Phi]}{\delta \Phi^2} + R_k^\Phi} \right)_{\phi\phi/q\bar{q}}, \quad (3)$$

with $\Phi = (q, \bar{q}, \phi)$ denoting all species of fields.

Inserting the effective action in Eq. (1) into the flow equation (2), one arrives at the flow equation for the effective potential, which reads

$$\begin{aligned} \partial_t V_k(\rho) = & \frac{k^4}{4\pi^2} \left[(N_f^2 - 1) l_0^{(B,4)}(\bar{m}_{\pi,k}^2, \eta_{\phi,k}^\perp, z_\phi; T) \right. \\ & + l_0^{(B,4)}(\bar{m}_{\sigma,k}^2, \eta_{\phi,k}^\perp, z_\phi; T) \\ & \left. - 4N_c N_f l_0^{(F,4)}(\bar{m}_{q,k}^2, \eta_{q,k}; T, \mu) \right], \end{aligned} \quad (4)$$

with the RG invariant dimensionless meson and quark masses as follows

$$\bar{m}_{\pi,k}^2 = \frac{V_k'(\rho)}{k^2 Z_{\phi,k}^\perp}, \quad \bar{m}_{\sigma,k}^2 = \frac{V_k'(\rho) + 2\rho V_k''(\rho)}{k^2 Z_{\phi,k}^\perp}, \quad (5)$$

$$\bar{m}_{q,k}^2 = \frac{h_k^2 \rho}{2k^2 Z_{q,k}^2}. \quad (6)$$

The threshold functions $l_0^{(B)}$ and $l_0^{(F)}$ are presented in Eqs. (B16) and (B17), and the anomalous dimensions for the mesons and quark are defined as

$$\eta_{\phi,k}^\perp = -\frac{\partial_t Z_{\phi,k}^\perp}{Z_{\phi,k}^\perp}, \quad \eta_{\phi,k}^\parallel = -\frac{\partial_t Z_{\phi,k}^\parallel}{Z_{\phi,k}^\parallel}, \quad \eta_{q,k} = -\frac{\partial_t Z_{q,k}}{Z_{q,k}}. \quad (7)$$

Note that $z_\phi \equiv Z_{\phi,k}^\parallel / Z_{\phi,k}^\perp$ enters into the flow of $V_k(\rho)$ through the mesonic fluctuations as shown in Eq. (4).

The transversal anomalous dimension for the π -meson is obtained by employing the projection as follows

$$\eta_{\phi,k}^\perp = -\frac{1}{3Z_{\phi,k}^\perp} \delta_{ij} \frac{\partial}{\partial(|\mathbf{p}|^2)} \frac{\delta^2 \partial_t \Gamma_k}{\delta \pi_i(-p) \delta \pi_j(p)} \Big|_{\substack{p_0=0 \\ \mathbf{p}=0}}, \quad (8)$$

and the longitudinal one reads

$$\eta_{\phi,k}^\parallel = -\frac{1}{3Z_{\phi,k}^\parallel} \delta_{ij} \frac{\partial}{\partial(p_0^2)} \frac{\delta^2 \partial_t \Gamma_k}{\delta \pi_i(-p) \delta \pi_j(p)} \Big|_{\substack{p_0=0 \\ \mathbf{p}=0}}. \quad (9)$$

Their explicit expressions are given in Eqs. (A1) and (A2), respectively. The difference of the anomalous dimension between the π and σ mesons is neglected here. Note that even they are different, choosing the π -meson anomalous dimension for η_ϕ , as done in this work, could minimize the errors of calculation, at least when the baryon chemical potential is not very high, since the mass of the pion is less than that of σ -meson, because of its nature of Goldstone particle, and the number of the degree of freedom for the pion is also larger. But we should mention that, in the region of the high baryon chemical potential in the phase diagram, especially near the CEP,

the σ -mode is the most relevant collective mode and the mass of the σ -meson is vanishing, it is necessary to distinguish the anomalous dimensions of π and σ , which will be investigated in the future.

The anomalous dimension for the quark is obtained by projecting the inverse quark propagator onto the vector channel, as follows

$$\eta_q(p_0, \mathbf{p}) = \frac{1}{4Z_{q,k}(p_0, \mathbf{p})} \times \text{Re} \left[\frac{\partial}{\partial(|\mathbf{p}|^2)} \text{tr} \left(i\gamma \cdot \mathbf{p} \left(-\frac{\delta^2}{\delta\bar{q}(p)\delta q(p)} \partial_t \Gamma_k \right) \right) \right] \Big|_{\substack{p_0, ex \\ \mathbf{p}=0}}. \quad (10)$$

where the spacial component of the external momentum is chosen to be vanishing, as same as the mesonic anomalous dimensions in Eqs. (8) and (9). Note that because of the fermionic property of the quark, its lowest Matsubara frequency is nonvanishing, and we denote it here as $p_{0,ex}$, which is described in Appendix A. Projecting of the inverse quark propagator onto the scalar channel leads us to the flow of the Yukawa coupling [2], which reads

$$\partial_t h_k(\rho) = \frac{1}{2\sigma} \text{Re} \left[\text{tr} \left(-\frac{\delta^2}{\delta\bar{q}(p)\delta q(p)} \partial_t \Gamma_k \right) \right] \Big|_{\substack{p_0, ex \\ \mathbf{p}=0}}. \quad (11)$$

The analytic expressions of Eq. (10) and Eq. (11) are given in Eq. (A3) and Eq. (A4), respectively.

III. EQUATION OF STATE AND BARYON NUMBER FLUCTUATIONS

In the PQM model (1) the thermodynamical potential density reads

$$\Omega[T, \mu] = V_{k=0}(\rho) - c\sigma + V_{\text{glue}}(L, \bar{L}), \quad (12)$$

where all the fields are on their respective equations of motion. L is the traced Polyakov loop and \bar{L} is its complex conjugate. They are related to the temporal gluonic background field A_0 in Eq. (1) through the equations as follows

$$L(\mathbf{x}) = \frac{1}{N_c} \langle \text{Tr } \mathcal{P}(\mathbf{x}) \rangle, \quad \bar{L}(\mathbf{x}) = \frac{1}{N_c} \langle \text{Tr } \mathcal{P}^\dagger(\mathbf{x}) \rangle, \quad (13)$$

with the Polyakov loop $\mathcal{P}(\mathbf{x})$ which reads

$$\mathcal{P}(\mathbf{x}) = \mathcal{P} \exp \left(ig \int_0^\beta d\tau A_0(\mathbf{x}, \tau) \right), \quad (14)$$

where the path-ordering operator \mathcal{P} has been employed.

In this work we employ the polynomial parametrization of the glue potential [6], which reads

$$\bar{V}_{\text{glue}}(L, \bar{L}) = -\frac{b_2(T)}{2} L\bar{L} - \frac{b_3}{6} (L^3 + \bar{L}^3) + \frac{b_4}{4} (L\bar{L})^2, \quad (15)$$

with the dimensionless glue potential $\bar{V}_{\text{glue}} = V_{\text{glue}}/T^4$. The temperature dependence of the glue potential is encoded in the coefficient of the quadratic term in the Polyakov loop, to wit,

$$b_2(T) = a_1 + \frac{a_2}{1+t_r} + \frac{a_3}{(1+t_r)^2} + \frac{a_4}{(1+t_r)^3}, \quad (16)$$

with the reduced temperature $t_r = (T - T_c)/T_c$. The parameters in the glue potential are determined by fitting the thermodynamics and the Polyakov loop dynamics in the Yang-Mills (YM) theory, which are $a_1 = 6.75$, $a_2 = -1.95$, $a_3 = 2.625$, $a_4 = -7.44$, $b_3 = 0.75$, and $b_4 = 7.5$. It has been found that the unquenched effect on the glue potential in QCD is well captured from that in the YM theory [7], by employing the rescale for the reduced temperature as follows

$$(t_r)_{\text{YM}} \rightarrow \alpha (t_r)_{\text{glue}}, \quad (17)$$

with

$$(t_r)_{\text{glue}} = (T - T_c^{\text{glue}})/T_c^{\text{glue}}, \quad (18)$$

and $\alpha \simeq 0.57$. In this work we adopt $T_c^{\text{glue}} = 208$ MeV for $N_f = 2$ flavor QCD, which is obtained from the renormalization group analysis in QCD, see [8] for details.

The pressure and the energy density are given by

$$p = -\Omega[T, \mu], \quad (19)$$

$$\varepsilon = -p + Ts + \sum_{i=u,d} \mu_i n_i, \quad (20)$$

with the entropy density and quark number density reading

$$s = \frac{\partial p}{\partial T} \quad \text{and} \quad n_i = \frac{\partial p}{\partial \mu_i}, \quad (21)$$

respectively. The interaction measure or the trace anomaly is given as follows

$$\Delta = \varepsilon - 3p. \quad (22)$$

In this work we will also investigate the fluctuations of the baryon and quark numbers, which are obtained through high-order derivatives of the pressure w.r.t. their respective chemical potentials. Taking the baryon number fluctuations for instance, the n -th order one reads

$$\chi_n^B = \frac{\partial^n}{\partial(\mu_B/T)^n} \frac{p}{T^4}, \quad (23)$$

which is also called as the n -th order generalized susceptibility of the baryon number. χ_n^B 's in Eq. (23) are related to the cumulants of the baryon number distribu-

tions, e.g.,

$$\chi_1^B = \frac{1}{VT^3} \langle N_B \rangle, \quad (24)$$

$$\chi_2^B = \frac{1}{VT^3} \langle (\delta N_B)^2 \rangle, \quad (25)$$

$$\chi_3^B = \frac{1}{VT^3} \langle (\delta N_B)^3 \rangle, \quad (26)$$

$$\chi_4^B = \frac{1}{VT^3} \left(\langle (\delta N_B)^4 \rangle - 3 \langle (\delta N_B)^2 \rangle^2 \right), \quad (27)$$

up to the fourth order. Here $\langle \dots \rangle$ denotes the ensemble average and $\delta N_B = N_B - \langle N_B \rangle$.

IV. NUMERICAL CALCULATIONS AND RESULTS

We employ the approach of Taylor expansion to solve the flow of the effective potential in Eq. (4) numerically. Expanding around the expansion point κ , one is led to

$$V_k(\rho) = \sum_{n=0}^{N_v} \frac{\lambda_{n,k}}{n!} (\rho - \kappa_k)^n, \quad (28)$$

where a subscript k is affixed to the expansion point κ , indicating that the expansion point can be RG scale dependent, and N_v is the highest order which is included in the calculations. The convergency is obtained when the calculated results are almost no longer influenced by the increment of N_v , after it is above some value. We adopt two commonly used expansion approaches in the literatures. It is more convenient to work with the renormalized variables, to wit,

$$\bar{V}_k(\bar{\rho}) = \sum_{n=0}^{N_v} \frac{\bar{\lambda}_{n,k}}{n!} (\bar{\rho} - \bar{\kappa}_k)^n, \quad (29)$$

with $\bar{V}_k(\bar{\rho}) = V_k(\rho)$, $\bar{\lambda}_{n,k} = \lambda_{n,k} / (Z_{\phi,k}^\perp)^n$, $\bar{\rho} = Z_{\phi,k}^\perp \rho$, and $\bar{\kappa}_k = Z_{\phi,k}^\perp \kappa_k$. Inserting Eq. (29) into its flow equation (4), one is led to

$$\begin{aligned} & \partial_{\bar{\rho}}^n \left(\partial_t \big|_{\bar{\rho}} \bar{V}_k(\bar{\rho}) \right) \Big|_{\bar{\rho}=\bar{\kappa}_k} \\ &= (\partial_t - n\eta_{\phi,k}^\perp) \bar{\lambda}_{n,k} - (\partial_t \bar{\kappa}_k + \eta_{\phi,k}^\perp \bar{\kappa}_k) \bar{\lambda}_{n+1,k}. \end{aligned} \quad (30)$$

Two different expansion approaches are commonly used in the literature: one is the fixed bare expansion point with $\partial_t \kappa_k = 0$, i.e., κ_k is independent of the scale, which yields

$$\partial_t \bar{\kappa}_k + \eta_{\phi,k}^\perp \bar{\kappa}_k = 0. \quad (31)$$

It follows immediately that the second term on the r.h.s. of Eq. (30) is vanishing for the fixed point expansion.

Consequently, $\bar{\lambda}_{n,k}$'s of different orders are decoupled and there is no feedback from the high order coupling to low order flows. Therefore, the convergency property is well controlled in the fixed point expansion. For more discussions about the fixed point expansion, see, e.g. [2]. Another approach is the running physical expansion, which demands that the expansion point is the solution of equation of motion for every value of k , to wit,

$$\frac{\partial}{\partial \bar{\rho}} \left(\bar{V}_k(\bar{\rho}) - \bar{c}_k (2\bar{\rho})^{\frac{1}{2}} \right) \Big|_{\bar{\rho}=\bar{\kappa}_k} = 0, \quad (32)$$

with $\bar{c}_k = c / (Z_{\phi,k}^\perp)^{1/2}$ being the renormalized strength of the explicit chiral symmetry breaking in the effective action (1). Note that the bare c is scale independent, thus one has $\partial_t \bar{c}_k = (1/2) \eta_{\phi,k}^\perp \bar{c}_k$. Combining Eq. (30) and Eq. (32), one arrives at the flow of the physical expansion point, which reads

$$\begin{aligned} \partial_t \bar{\kappa}_k &= - \frac{\bar{c}_k^2}{\bar{\lambda}_{1,k}^3 + \bar{c}_k^2 \bar{\lambda}_{2,k}} \left[\partial_{\bar{\rho}} \left(\partial_t \big|_{\bar{\rho}} \bar{V}_k(\bar{\rho}) \right) \Big|_{\bar{\rho}=\bar{\kappa}_k} \right. \\ &\quad \left. + \eta_{\phi,k}^\perp \left(\frac{\bar{\lambda}_{1,k}}{2} + \bar{\kappa}_k \bar{\lambda}_{2,k} \right) \right]. \end{aligned} \quad (33)$$

In this work, we will investigate the influence of these two expansion approaches on the fluctuations of the baryon number.

Furthermore, we also use the Taylor expansion to include the field dependence of the Yukawa coupling, which reads

$$\bar{h}_k(\bar{\rho}) = \sum_{n=0}^{N_h} \frac{\bar{h}_{n,k}}{n!} (\bar{\rho} - \bar{\kappa}_k)^n, \quad (34)$$

with

$$\bar{h}_k(\bar{\rho}) = \frac{h_k(\rho)}{Z_{q,k} (Z_{\phi,k}^\perp)^{1/2}}, \quad \text{and} \quad \bar{h}_{n,k} = \frac{h_{n,k}}{Z_{q,k} (Z_{\phi,k}^\perp)^{(2n+1)/2}}, \quad (35)$$

where N_h is the order, up to which the Taylor expansion of $\bar{h}_k(\bar{\rho})$ is done. Inserting Eq. (35) into Eq. (11), one is led to

$$\begin{aligned} & \partial_{\bar{\rho}}^n \left(\partial_t \big|_{\bar{\rho}} \bar{h}_k(\bar{\rho}) \right) \Big|_{\bar{\rho}=\bar{\kappa}_k} \\ &= (\partial_t - n\eta_{\phi,k}^\perp) \bar{h}_{n,k} - (\partial_t \bar{\kappa}_k + \eta_{\phi,k}^\perp \bar{\kappa}_k) \bar{h}_{n+1,k}, \end{aligned} \quad (36)$$

through which the Yukawa couplings of high orders can be solved.

It is left to specify the parameters in the low energy effective models: the UV cutoff is chosen to be $\Lambda = 700$ MeV; the effective potential at $k = \Lambda$ is parameterized as follows

$$V_\Lambda(\rho) = \frac{\lambda_\Lambda}{2} \rho^2 + \nu_\Lambda \rho, \quad (37)$$

with $\lambda_\Lambda = 10$ and $\nu_\Lambda = (0.556 \text{ GeV})^2$. Furthermore, the strength of the explicit chiral symmetry breaking in (1) is $c = 1.97 \times 10^{-3} (\text{GeV})^3$, and the Yukawa coupling is $h_\Lambda = 7.33$. Employing the fixed point expansion and all the truncations discussed in this work, including the splitting of the meson wave function renormalization and the field dependent Yukawa coupling, etc., we obtain the physical observables in the vacuum, which read $f_\pi = 92 \text{ MeV}$, $m_q = 300 \text{ MeV}$, $m_\pi = 136 \text{ MeV}$, and $m_\sigma = 454 \text{ MeV}$. Note that this is the only set of parameters we use in this work, even they result in some quantitative change of the observables in the vacuum by adopting other truncations discussed in the following. We will not tune these parameters to match the physical observables in the vacuum for different truncations, which would facilitate the comparisons among different truncations.

I am here

A. The flow equations of the effective potential and the Yukawa coupling

B. Baryon number fluctuation and kurtosis

There are many ways to determine the freeze-out temperature.

$\sqrt{s} (\text{GeV})$	200	62.4	39	27	19.6	11.5	7.7
$\mu_{B,N_f=2} (\text{MeV})$	25.3	78.1	121	168.7	222.7	343	459.4

TABLE I. The relationship of collision energy and baryon chemical potential

V. NUMERICAL RESULTS AND CONCLUSION

These four parameters are chosen by fitting the observables: $m_\pi = 135.9 \text{ MeV}$, $m_\sigma = 460.0 \text{ MeV}$, $f_\pi = 92.1 \text{ MeV}$, $m_q = 298.8 \text{ MeV}$.

In the end, we give the numerical calculation results of the physical quantity. In this section we will show the results of the comparison in the two flavor PQM model. Two comparisons have been made, one is $Z_\phi^\parallel = Z_\phi^\perp$ and $Z_\phi^\parallel \neq Z_\phi^\perp$, the other one is the fix point and physical point expansion of the effective potential.

As we can see in the Fig. IV, the pion mass and constituent quark mass as the function of temperature. It is clear that the pion mass under the physical point is larger at the high temperature, which means the pion is decoupling quicker. For the meson mass is related to the expansion of the effective potential, the expansion point is running with the cutoff scale k or not will of course influence the value of the pion mass. However, the split of the meson wave function renormalisation make little effect on the mass.

As is shown in the Fig. IV B, because the baryon chemical potential has little influence to the numerical result

of the χ_2^B and χ_4^B , however the χ_1^B and χ_3^B are more sensitive to the chemical potential. Consequently, we give the odd order of the fluctuation under the chemical potential of 50 MeV and 100 MeV, and the even order under vanishing chemical potential. The results of the quartic fluctuations under two kinds of wave function renormalizations have larger difference at the peak of the curves, the results of $Z_{\phi,k}^\perp \neq Z_{\phi,k}^\parallel$ are little lower than the results of $Z_{\phi,k}^\perp = Z_{\phi,k}^\parallel$.

In the Fig. 3 we show $\kappa\sigma^2 = \chi_4^B/\chi_2^B$ the kurtosis of the baryon number fluctuation. We can tell from the curves, the two kinds of Z_ϕ almost no effect on the kurtosis results. On the other hand, the influence of the running expansion point of the effective potential is greater. The physical point expansion suppress the kurtosis quicker as the temperature rises than the fix point expansion. It is expected from the results of the four order of the fluctuation.

In the Fig. V we give the pion decay constant and trace anomaly as a function of temperature. The left one is the pion decay constant. It is clear, the separation of the meson wave function renormalisation doesn't make much change. However, the running expansion point of the effective potential brings some differences at high temperature. The trace anomaly doesn't change much either under the different wave function renormalisation, and the physical point expansion suppress the value at high temperature.

ACKNOWLEDGMENTS

Thanks

Appendix A: Anomalous dimensions and Yukawa coupling

Inserting the effective action in Eq. (1) and its the flow equation in Eq. (2) into Eq. (8), and employing the $3d$ - regulators in Eq. (B1) and Eq. (B2), one obtains the transversal anomalous dimension for the meson, as follows

$$\eta_{\phi,k}^\perp = \frac{1}{6\pi^2} \left\{ \frac{4}{k^2 z_\phi^4} \bar{\kappa}_k (\bar{V}_k''(\bar{\kappa}_k))^2 \mathcal{B}\mathcal{B}_{(2,2)}(\bar{m}_{\pi,k}^2, \bar{m}_{\sigma,k}^2; T) \right. \\ \left. + N_c \bar{h}_k^2 \left[\mathcal{F}_{(2)}(\bar{m}_{q,k}^2; T, \mu) (2\eta_{q,k} - 3) \right. \right. \\ \left. \left. - 4(\eta_{q,k} - 2) \mathcal{F}_{(3)}(\bar{m}_{q,k}^2; T, \mu) \right] \right\}, \quad (\text{A1})$$

and relevant threshold functions are given in Appendix B. In the same way, the longitudinal anomalous dimension

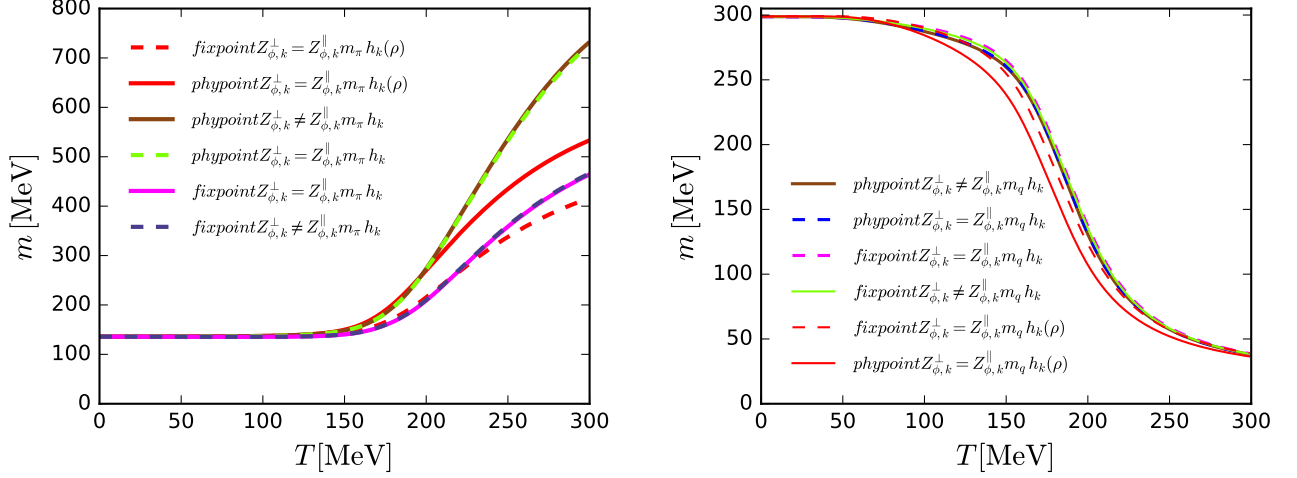


FIG. 1. The left diagram is the mass of the pion as a function of temperature, the right curves are the constituent quark mass. These diagrams are obtained under fix point and physical point expansion of the effective potential.

for the meson in Eq. (9) reads

$$\begin{aligned} \eta_{\phi,k}^{\parallel} = & \frac{1}{6\pi^2} \left\{ \frac{4}{k^2 z_{\phi}^4} \bar{\kappa}_k (\bar{V}_k''(\bar{\kappa}_k))^2 \left[-6\mathcal{BB}_{(2,2)}(\bar{m}_{\pi,k}^2, \bar{m}_{\sigma,k}^2; T) \right. \right. \\ & + \frac{4}{z_{\phi}} (1 + \bar{m}_{\sigma}^2) \mathcal{BB}_{(2,3)}(\bar{m}_{\pi,k}^2, \bar{m}_{\sigma,k}^2; T) \\ & \left. \left. + \frac{4}{z_{\phi}} (1 + \bar{m}_{\pi}^2) \mathcal{BB}_{(3,2)}(\bar{m}_{\pi,k}^2, \bar{m}_{\sigma,k}^2; T) \right] \right. \\ & \left. \times \left(1 - \frac{1}{5} \eta_{\phi,k}^{\perp} \right) + \frac{N_c \bar{h}_k^2}{z_{\phi}} \mathcal{F}_{(3)}(\bar{m}_{q,k}^2; T, \mu) (4 - \eta_{q,k}) \right\}, \end{aligned} \quad (\text{A2})$$

The anomalous dimension for the quark in Eq. (10) is given by

$$\begin{aligned} \eta_{q,k} = & \frac{1}{24\pi^2 N_f} (4 - \eta_{\phi,k}^{\perp}) \bar{h}_k^2 \\ & \times \left\{ (N_f^2 - 1) \mathcal{FB}_{(1,2)}(\bar{m}_{q,k}^2, \bar{m}_{\pi,k}^2; T, \mu, p_{0,ex}) \right. \\ & \left. + \mathcal{FB}_{(1,2)}(\bar{m}_{q,k}^2, \bar{m}_{\sigma,k}^2; T, \mu, p_{0,ex}) \right\}, \end{aligned} \quad (\text{A3})$$

where $p_{0,ex} = \pi T$ for the finite temperature part and $[k^2 + (\pi T)^2 \exp\{-2k/(5T)\}]^{1/2}$ for the vacuum part in the threshold function \mathcal{FB} 's in Eq. (B23). Note that the modification of the lowest-order Matsubara frequency in the vacuum part is employed to suppress the artificial temperature dependence of thermodynamics in the low temperature regime, see e.g. [3, 9] for more discussions. The flow of the field-dependent Yukawa coupling

in Eq. (11) is firstly derived in [2] and is also presented here for convenience, which reads

$$\begin{aligned} \partial_t|_{\rho} \bar{h}_k(\bar{\rho}) = & \left(\frac{1}{2} \eta_{\phi,k} + \eta_{q,k} \right) \bar{h}_k(\bar{\rho}) \\ & + \frac{\bar{h}_k^3(\bar{\rho})}{4\pi^2 N_f} \left[L_{(1,1)}^{(4)}(\bar{m}_{q,k}^2, \bar{m}_{\sigma,k}^2, \eta_{q,k}, \eta_{\phi,k}^{\perp}; T, \mu, p_{0,ex}) \right. \\ & \left. - (N_f^2 - 1) L_{(1,1)}^{(4)}(\bar{m}_{q,k}^2, \bar{m}_{\pi,k}^2, \eta_{q,k}, \eta_{\phi,k}^{\perp}; T, \mu, p_{0,ex}) \right] \\ & + \frac{1}{2\pi^2} \bar{h}_k(\bar{\rho}) \bar{h}_k'(\bar{\rho}) \bar{\rho} \left[\bar{h}_k(\bar{\rho}) + \bar{\rho} \bar{h}_k'(\bar{\rho}) \right] \\ & \times L_{(1,1)}^{(4)}(\bar{m}_{q,k}^2, \bar{m}_{\sigma,k}^2, \eta_{q,k}, \eta_{\phi,k}^{\perp}; T, \mu, p_{0,ex}) \\ & - \frac{k^2}{4\pi^2} \left[(3\bar{h}_k'(\bar{\rho}) + 2\bar{\rho} \bar{h}_k''(\bar{\rho})) l_1^{(B,4)}(\bar{m}_{\sigma,k}^2, \eta_{\phi,k}^{\perp}; T) \right. \\ & \left. + 3\bar{h}_k'(\bar{\rho}) l_1^{(B,4)}(\bar{m}_{\pi,k}^2, \eta_{\phi,k}^{\perp}; T) \right]. \end{aligned} \quad (\text{A4})$$

Appendix B: Threshold functions

In this work we use the 3d- flat or Litim regulators [10, 11], which are very suited for the computations at finite temperature and densities, since the summation for the Matsubara frequencies is not affected by the 3d regulators, and can be performed analytically. The regulators

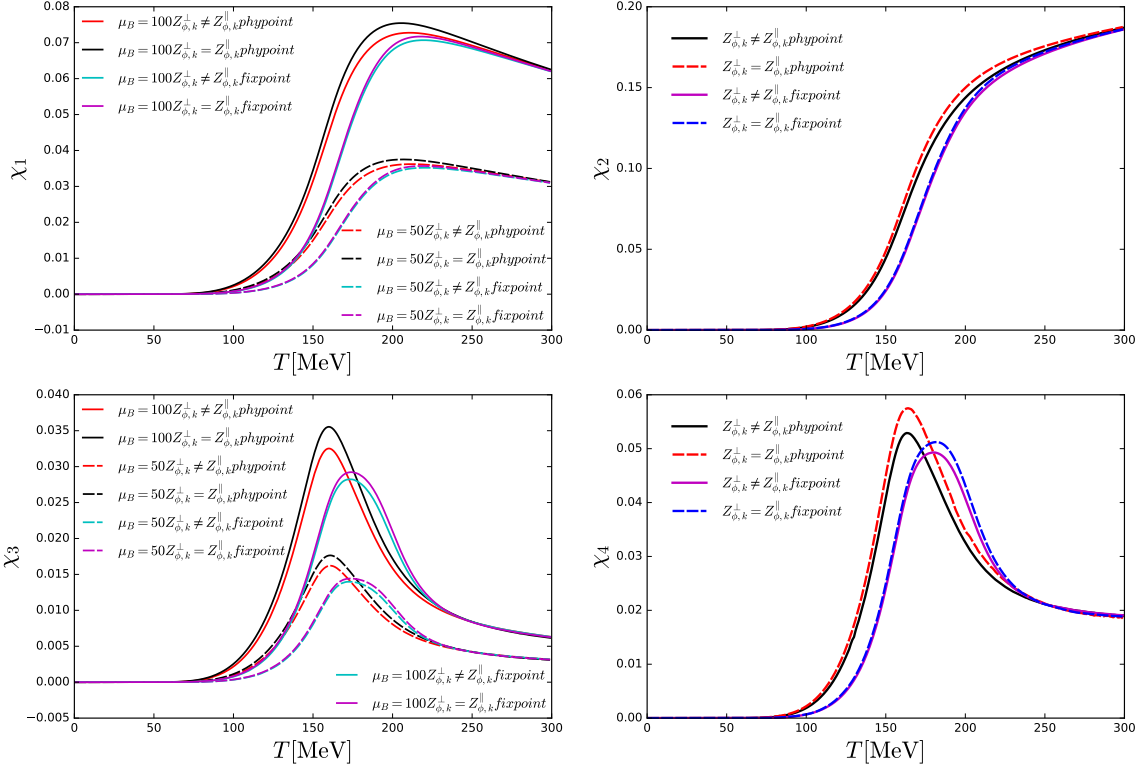


FIG. 2. The first to the fourth order of the baryon number fluctuation, which are obtained under $Z_{\phi}^{\parallel} = Z_{\phi}^{\perp}$, $Z_{\phi}^{\parallel} \neq Z_{\phi}^{\perp}$ and fix point, physical point expansion of the effective potential.

in Eq. (2) read

$$R_k^{\phi}(q_0, \mathbf{q}) = Z_{\phi,k}^{\perp} \mathbf{q}^2 r_B(\mathbf{q}^2/k^2), \quad (\text{B1})$$

$$R_k^q(q_0, \mathbf{q}) = Z_{q,k} i\gamma \cdot \mathbf{q} r_F(\mathbf{q}^2/k^2), \quad (\text{B2})$$

with

$$r_B(x) = \left(\frac{1}{x} - 1 \right) \Theta(1-x), \quad (\text{B3})$$

$$r_F(x) = \left(\frac{1}{\sqrt{x}} - 1 \right) \Theta(1-x), \quad (\text{B4})$$

where $\Theta(x)$ is the Heaviside step function. Note that since $Z_{\phi,k}^{\perp} \neq Z_{\phi,k}^{\parallel}$, it is the transversal wave function renormalization for the meson appearing in Eq. (B1).

In the threshold functions we usually need the dimensionless meson and quark propagators as follows

$$G_{\phi}(q, \bar{m}_{\phi,k}^2) = \frac{1}{z_{\phi} \tilde{q}_0^2 + 1 + \bar{m}_{\phi,k}^2}, \quad (\text{B5})$$

$$G_q(q, \bar{m}_{q,k}^2) = \frac{1}{(\tilde{q}_0 + i\tilde{\mu})^2 + 1 + \bar{m}_{q,k}^2}, \quad (\text{B6})$$

with $\tilde{\mu} = \mu/k$ and $\tilde{q}_0 = q_0/k$, where the Matsubara frequency is $q_0 = 2n_q\pi T$ for bosons and $(2n_q + 1)\pi T$ for fermions with $n_q \in \mathbb{Z}$.

The definition of the threshold functions $\mathcal{B}_{(n)}$ and $\mathcal{F}_{(n)}$ is given by

$$\mathcal{B}_{(n)}(\bar{m}_{\phi,k}^2; T) = \frac{T}{k} \sum_{n_q} \left(G_{\phi}(q, \bar{m}_{\phi,k}^2) \right)^n, \quad (\text{B7})$$

$$\mathcal{F}_{(n)}(\bar{m}_{q,k}^2; T, \mu) = \frac{T}{k} \sum_{n_q} \left(G_q(q, \bar{m}_{q,k}^2) \right)^n. \quad (\text{B8})$$

After performing the Matsubara sum, one arrives at

$$\mathcal{B}_{(1)}(\bar{m}_{\phi,k}^2; T) = \frac{1}{\sqrt{z_{\phi}(1 + \bar{m}_{\phi,k}^2)}} \left(\frac{1}{2} + n_B(\bar{m}_{\phi,k}^2, z_{\phi}; T) \right), \quad (\text{B9})$$

and

$$\mathcal{F}_{(1)}(\bar{m}_{q,k}^2; T, \mu) = \frac{1}{2\sqrt{1 + \bar{m}_{q,k}^2}} \times \left(1 - n_F(\bar{m}_{q,k}^2; T, \mu) - n_F(\bar{m}_{q,k}^2; T, -\mu) \right), \quad (\text{B10})$$

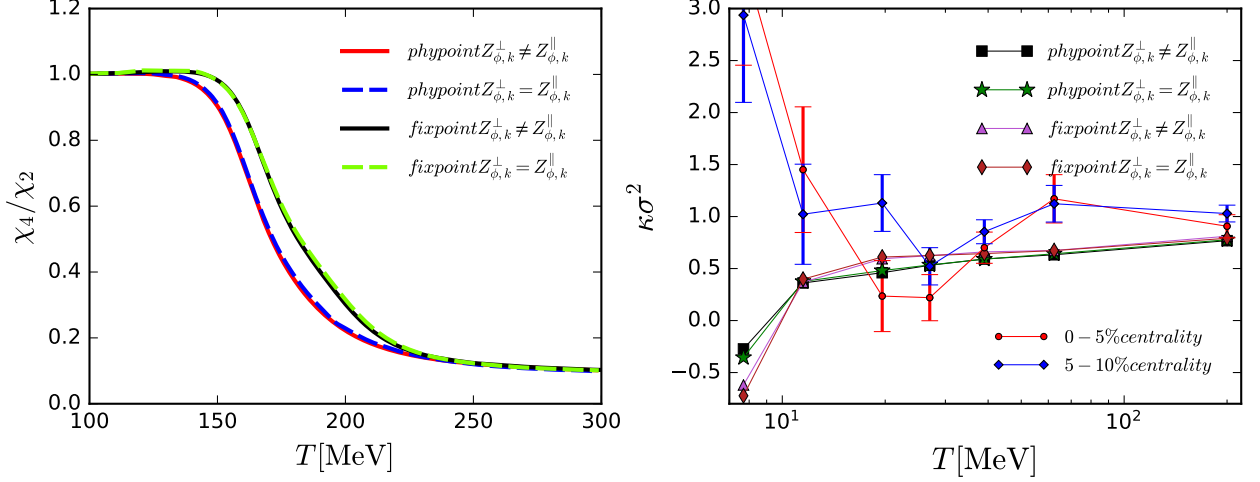


FIG. 3. The left curves are the kurtosis as the function of temperature. The right broken lines are the kurtosis as the function of collision energy.

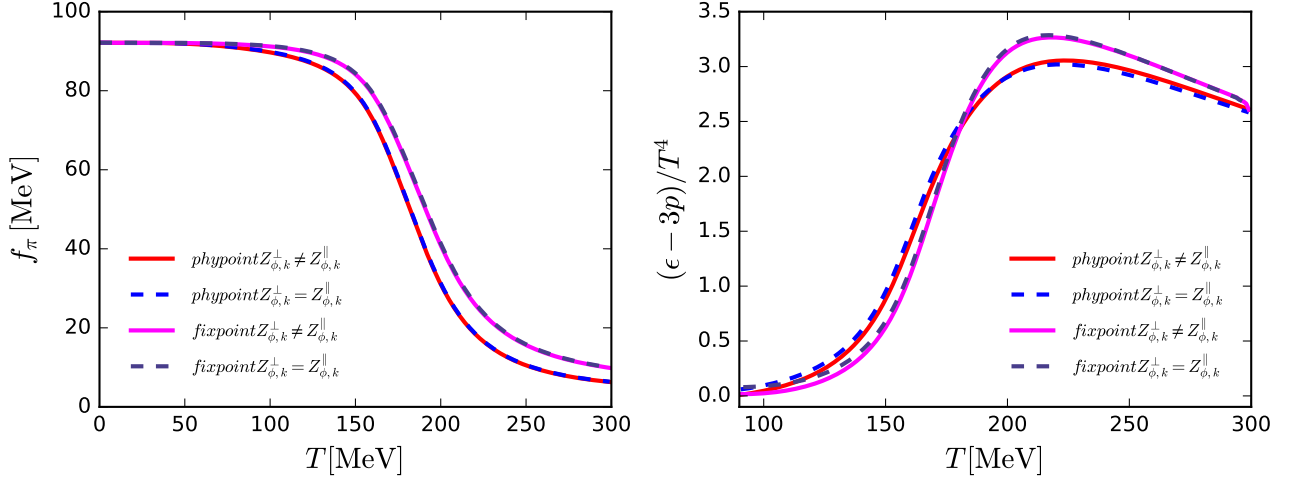


FIG. 4.

with the bosonic and fermionic distribution functions being

$$n_B(\bar{m}_{\phi,k}^2; z_\phi; T) = \frac{1}{\exp \left\{ \frac{1}{T} \frac{k}{z_\phi^{1/2}} \sqrt{1 + \bar{m}_{\phi,k}^2} \right\} - 1}, \quad (\text{B11})$$

and

$$n_F(\bar{m}_{q,k}^2; T, \mu) = \frac{1}{\exp \left\{ \frac{1}{T} \left[k \sqrt{1 + \bar{m}_{q,k}^2} - \mu \right] \right\} + 1}. \quad (\text{B12})$$

Note that when the Polaykov loop is taken into account,

the fermionic distribution function is modified as follows

$$n_F(\bar{m}_{q,k}^2; T, \mu, L, \bar{L}) = \frac{1 + 2\bar{L}e^{x/T} + Le^{2x/T}}{1 + 3\bar{L}e^{x/T} + 3Le^{2x/T} + e^{3x/T}}, \quad (\text{B13})$$

with $x = k \sqrt{1 + \bar{m}_{q,k}^2} - \mu$, and $n_F(\bar{m}_{q,k}^2; T, -\mu)$ in Eq. (B10) is replaced with $n_F(\bar{m}_{q,k}^2; T, -\mu, \bar{L}, L)$ accordingly. With Eq. (B9) and Eq. (B10), high-order threshold functions in Eqs. (B7) and (B8) are readily obtained as

$$\mathcal{B}_{(n+1)}(\bar{m}_{\phi,k}^2; T) = -\frac{1}{n} \frac{\partial}{\partial \bar{m}_{\phi,k}^2} \mathcal{B}_{(n)}(\bar{m}_{\phi,k}^2; T), \quad (\text{B14})$$

$$\mathcal{F}_{(n+1)}(\bar{m}_{q,k}^2; T, \mu) = -\frac{1}{n} \frac{\partial}{\partial \bar{m}_{q,k}^2} \mathcal{F}_{(n)}(\bar{m}_{q,k}^2; T, \mu). \quad (\text{B15})$$

The threshold functions in the flow of effective potential in Eq. (4) are given by

$$\begin{aligned} l_0^{(B,d)}(\bar{m}_{\phi,k}^2, \eta_{\phi,k}^\perp, z_\phi; T) \\ = \frac{2}{d-1} \left(1 - \frac{\eta_{\phi,k}^\perp}{d+1} \right) \mathcal{B}_{(1)}(\bar{m}_{\phi,k}^2, z_\phi; T), \end{aligned} \quad (\text{B16})$$

and

$$\begin{aligned} l_0^{(F,d)}(\bar{m}_{q,k}^2, \eta_{q,k}, T, \mu) \\ = \frac{2}{d-1} \left(1 - \frac{\eta_{q,k}}{d} \right) \mathcal{F}_{(1)}(\bar{m}_{q,k}^2, T, \mu). \end{aligned} \quad (\text{B17})$$

In Eq. (A4), one also needs $l_1^{(B,4)}$, which is obtained from

$$l_1^{(B/F,d)}(m^2) = - \frac{\partial}{\partial m^2} l_0^{(B/F,d)}(m^2). \quad (\text{B18})$$

Furthermore, we also need other threshold functions, such as

$$\begin{aligned} \mathcal{B}\mathcal{B}_{(n_1, n_2)}(m_1^2, m_2^2; T) \\ = \frac{T}{k} \sum_{n_q} \left(G_\phi(q, \bar{m}_{\phi_a, k}^2) \right)^{n_1} \left(G_\phi(q, \bar{m}_{\phi_b, k}^2) \right)^{n_2}. \end{aligned} \quad (\text{B19})$$

in the expressions of the mesonic anomalous dimension in Eqs. (8) and (9). Inserting Eq. (B5) into Eq. (B19),

one is led to

$$\begin{aligned} \mathcal{B}\mathcal{B}_{(1,1)}(\bar{m}_{\phi_a, k}^2, \bar{m}_{\phi_b, k}^2; T) \\ = - \frac{1}{z_\phi^{1/2}} \left\{ \left(\frac{1}{2} + n_B(\bar{m}_{\phi_a, k}^2, z_\phi; T) \right) \frac{1}{(1 + \bar{m}_{\phi_a, k}^2)^{1/2}} \right. \\ \times \frac{1}{\bar{m}_{\phi_a, k}^2 - \bar{m}_{\phi_b, k}^2} + \left(\frac{1}{2} + n_B(\bar{m}_{\phi_b, k}^2, z_\phi; T) \right) \\ \times \frac{1}{(1 + \bar{m}_{\phi_b, k}^2)^{1/2}} \frac{1}{\bar{m}_{\phi_b, k}^2 - \bar{m}_{\phi_a, k}^2} \left. \right\}. \end{aligned} \quad (\text{B20})$$

In the same way, one could obtain higher-order ones by employing, e.g.,

$$\begin{aligned} \mathcal{B}\mathcal{B}_{(n_1+1, n_2)}(\bar{m}_{\phi_a, k}^2, \bar{m}_{\phi_b, k}^2; T) \\ = - \frac{1}{n_1} \frac{\partial}{\partial \bar{m}_{\phi_a, k}^2} \mathcal{B}\mathcal{B}_{(n_1, n_2)}(\bar{m}_{\phi_a, k}^2, \bar{m}_{\phi_b, k}^2; T). \end{aligned} \quad (\text{B21})$$

In the flow of the Yukawa coupling in (11), the threshold function L is introduced, which reads

$$\begin{aligned} L_{(1,1)}^{(4)}(\bar{m}_{q,k}^2, \bar{m}_{\phi,k}^2, \eta_{q,k}, \eta_{\phi,k}; T, \mu, p_0) \\ = \frac{2}{3} \left[\left(1 - \frac{\eta_{\phi,k}^\perp}{5} \right) \mathcal{F}\mathcal{B}_{(1,2)}(\bar{m}_{q,k}^2, \bar{m}_{\phi,k}^2; T, \mu, p_0) \right. \\ \left. + \left(1 - \frac{\eta_{q,k}}{4} \right) \mathcal{F}\mathcal{B}_{(2,1)}(\bar{m}_{q,k}^2, \bar{m}_{\phi,k}^2; T, \mu, p_0) \right], \end{aligned} \quad (\text{B22})$$

where the fermionic and bosonic mixing threshold functions $\mathcal{F}\mathcal{B}$'s are given by

$$\begin{aligned} \mathcal{F}\mathcal{B}_{(n_f, n_b)}(\bar{m}_{q,k}^2, \bar{m}_{\phi,k}^2; T, \mu, p_0) \\ = \frac{T}{k} \sum_{n_q} \left(G_q(q, \bar{m}_{q,k}^2) \right)^{n_f} \left(G_\phi(q-p, \bar{m}_{\phi,k}^2) \right)^{n_b}. \end{aligned} \quad (\text{B23})$$

The explicit expression for $\mathcal{F}\mathcal{B}_{(1,1)}$ is readily obtained after summing the Matsubara frequency, which can be found in, e.g. [3]. Higher-order $\mathcal{F}\mathcal{B}$'s are obtained from $\mathcal{F}\mathcal{B}_{(1,1)}$ by performing derivatives w.r.t. relevant masses as same as other threshold functions mentioned above.

-
- [1] B.-J. Schaefer and J. Wambach, Nucl. Phys. **A757**, 479 (2005), arXiv:nucl-th/0403039 [nucl-th].
[2] J. M. Pawłowski and F. Rennecke, Phys. Rev. **D90**, 076002 (2014), arXiv:1403.1179 [hep-ph].
[3] W.-j. Fu and J. M. Pawłowski, Phys. Rev. **D92**, 116006 (2015), arXiv:1508.06504 [hep-ph].
[4] A. J. Helmboldt, J. M. Pawłowski, and N. Strodthoff,

- Phys. Rev. **D91**, 054010 (2015), arXiv:1409.8414 [hep-ph].
[5] C. Wetterich, Phys. Lett. **B301**, 90 (1993).
[6] C. Ratti, M. A. Thaler, and W. Weise, Phys. Rev. **D73**, 014019 (2006), arXiv:hep-ph/0506234 [hep-ph].
[7] L. M. Haas, R. Stiele, J. Braun, J. M. Pawłowski, and J. Schaffner-Bielich, Phys. Rev. **D87**, 076004 (2013),

- arXiv:1302.1993 [hep-ph].
- [8] B.-J. Schaefer, J. M. Pawłowski, and J. Wambach, Phys. Rev. **D76**, 074023 (2007), arXiv:0704.3234 [hep-ph].
 - [9] W.-j. Fu, J. M. Pawłowski, F. Rennecke, and B.-J. Schaefer, Phys. Rev. **D94**, 116020 (2016), arXiv:1608.04302 [hep-ph].
 - [10] D. F. Litim, Phys. Lett. **B486**, 92 (2000), arXiv:hep-th/0005245 [hep-th].
 - [11] D. F. Litim, Phys. Rev. **D64**, 105007 (2001), arXiv:hep-th/0103195 [hep-th].